Taylor & Francis
Taylor & Francis Group

Chloromethylated Activated Carbon: A Useful New Synthon for Making a Novel Class of Sorbents for Heavy Metal Separations

William D. Samuels, Nikki H. LaFemina, Vichaya Sukwarotwat, Wassana Yantasee, Xiaohong S. Li, and Glen E. Fryxell
Pacific Northwest National Laboratory, Richland, WA, USA

The chloromethylation of activated carbon is described. Chloromethylation was found to produce a carbon derivative with a surface area of $1310 \, m^2/g$ and no significant change in the pore structure. The product was found to contain ~1.5 mmole of $-CH_2Cl$ groups per g of material, similar to the functional density reported in the original Merrifield resin synthesis. Displacement of the benzylic chloride was achieved by treating this material with an excess of sodium thiosulfate in refluxing aqueous methanol. The resulting Bunte salt was then hydrolyzed by treatment with warm 3 M HCl to afford the corresponding thiol ("AC-CH$_2$-SH") cleanly and in high yield. AC-CH$_2$-SH was found to be an effective heavy metal sorbent, efficiently capturing Hg, Pb, Ag, and Cu. Sorption kinetics were rapid, with equilibrium achieved in less than 30 minutes.

INTRODUCTION

Activated carbon is widely used world-wide, as a sorbent material for a wide variety of separation and purification needs. Activated carbon has also been modified to enhance its affinity for certain target species. For example, activated carbon has been impregnated with sulfur to enhance its affinity for Hg(1). This modification amounts to a simple intercalation/precipitation inside the carbon host, but it nonetheless has found significant application and use in industry. It is important to recognize that activated carbon can also be chemically modified through chemical reactions directed at the aromatic backbone, e.g., electrophilic aromatic substitution. For example, activated carbon has been nitrated (2,3). These $-NO_2$ groups can be reduced to form $-NH_2$ groups, which can then be used in amide coupling reactions, allowing the introduction of a wide variety of

ligands and/or functional groups. We have been interested in exploring this general area in more detail, to develop additional methods for chemical modification of activated carbon for chemically selective separations.

In the polymer realm, one of the single most versatile synthons is chloromethylated polystyrene, aka "Merrifield's resin" (4). The benzylic chloride in these swellable polymers is easily displaced, facilitating the synthesis of peptides, ion exchange resins, and catalyst supports (5–7). The chloromethylation reaction utilized in Merrifield's original synthesis involves the SnCl$_4$ catalyzed reaction of $ClCH_2-O-CH_3$ with crosslinked polystyrene, giving a product that contained approximately 1.89 mmole $-CH_2Cl$ per gram of resin (4) (currently available commercial versions of this polymer contain between 1.0 and 4.5 mmole Cl/g, depending on grade (8)). Chloromethylation reactions can be carried out in several ways, the most common being to treat the arene with formaldehyde, ZnCl$_2$, and HCl (9). The corresponding benzylic alcohol is an intermediate, which is then subsequently converted to the benzylic chloride by the HCl (as shown in Fig. 1). Crosslinking/polymerization (i.e., $Ar-CH_2-Ar$) can be a competing process with freely mobile substrates in solution.

The rigid, nanoporous architecture of activated carbon is well recognized, as is its excellent chemical and thermal stability (10). We were interested in applying this chloromethylation chemistry to the activated carbon backbone in an effort to create a useful synthon that could be easily modified for a variety of chemical separations. For our initial experiments, we wanted to make a high surface area support decorated with sulfur-based functionality so that we could use it as a part of our ongoing heavy metal sorbent studies (11). There are many ways that an alkyl halide can be converted to the corresponding thiol, but the most widely used strategy is to displace the halide with a sulfur-containing nucleophile (e.g., thiosulfate anion, thiourea, thioacetate, etc.), and then cleave the adduct to produce the thiol (see Fig. 2). This manuscript summarizes the synthesis of a novel nanoporous carbon-based sorbent
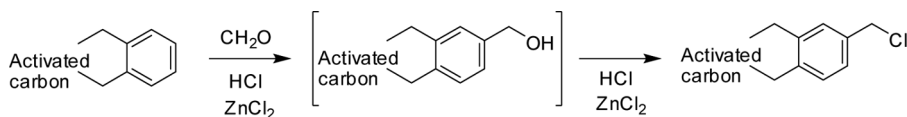
FIG. 1. A generic schematic outlining the chloromethylation of activated carbon.

material decorated with covalently anchored thiol groups, and demonstrates its efficacy for heavy metal separations.

EXPERIMENTAL

Activated carbon (Darco KB-B, 100 mesh) was purchased from Aldrich. This material was determined to have a surface area to mass ratio of $1483 \, m^2/g$, with a pore volume of $1.53 \, cc/g$. All other reagents were purchased from Aldrich and used as received.

Chloromethylation Procedure

A variation of the *Organic Synthesis* procedures was employed (12). A three neck, 500 mL round bottom flask was fitted with a large magnetic stir bar, one rubber septum, one short path condenser attached to a gas manifold with both a silicon oil bubbler and inert gas supply, and a glass dispersion tube connected to a tank of anhydrous HCl. The flask was charged first with 10.0 g of activated carbon, and 0.50 g (3.7 mmole) of zinc chloride, and finally with 250 mL of a 1:1 mixture of concentrated hydrochloric acid and acetic acid. The mixture was stirred at 27°C until all of the zinc chloride had dissolved, then the temperature was lowered to 0°C under an argon atmosphere and held at that temperature in an ice bath for the next three hours. After the mixture was at 0°C, the argon flow was stopped and HCl gas was vigorously bubbled through the suspension and then 38.0 g (0.47 mole) of 37% aq. formaldehyde was added all at once. The HCl flow was continued for an additional four hours, and then the solution was warmed to 27°C and stirred for an additional six hours. The chloromethylated activated carbon was collected on a glass frit, washed with two 100 mL portions of water, then three 100 mL portions of methanol. The cake was broken up and transferred to an open polyethylene container. The powder was further dried at 50°C and 0.25 atm for an additional 36 hr. The final dried product weighed 11.75 g.

The chloromethylated material had a surface area of $1310 \, m^2/g$ (consistent with a modest mass increase), and had a pore volume of $1.30 \, cc/g$. There was no discernable change in the pore structure, suggesting that the

chloromethylation chemistry had not blocked or significantly degraded the pore structure.

Elemental analysis of this material revealed a chlorine content of 5.21%, which corresponds to approximately 1.46 mmole/g. FTIR analysis of the chloromethylated material was inconclusive in terms of identifying new bands for the $-CH_2Cl$ group.

Thiosulfate Displacement

2.3865 g of the chloromethylated activated carbon was suspended in 60 mL methanol. Sodium thiosulfate (8.6 g, 35 mmole) was dissolved in 60 mL distilled water. The sodium thiosulfate solution was added to the chloromethylated activated carbon suspension in a 500 mL round bottom flask. This mixture was stirred under nitrogen and heated to reflux for total of 12 hours. The product was collected by vacuum filtration, washed copiously with distilled water, then with methanol. The product was then air dried for several days (1.549 g recovered).

BET surface area analysis revealed a surface area to mass ratio of $1179 \, m^2/g$, with no discernable difference in the pore size distribution from the chloromethylated activated carbon starting material. Once again, there was no evidence of damage to the pore structure of the activated carbon.

Elemental analysis of this material revealed a chlorine content of 0.15%, indicating efficient displacement of Cl. The S content was found to be 4.2%, consistent with the integration of thiosulfate anion into the product. This corresponds to 1.3 mmole S per gram of sorbent, or 0.65 mmole of thiosulfate/g. Given that this product started with 1.46 mmole of $-CH_2Cl$, this suggests ~45% conversion to the Bunte Salt. FTIR analysis of the chloromethylated material was inconclusive in terms of identifying new bands for the thiosulfate group (Bunte salts are known to have characteristic bands at $\sim 1215 \, cm^{-1}$, $\sim 1050 \, cm^{-1}$ and $\sim 650 \, cm^{-1}$ (13)).

Hydrolysis of Thiosulfate to Thiol

A 2.50 g sample of the above prepared chloromethylated activated carbon was suspended in 60 mL of methanol. Sodium thiosulfate (8.60 g; 34.7 mmole) was first dissolved in 60 mL of reverse osmosis (RO) water and then added to the reaction vessel containing the activated carbon. The mixture was refluxed for 2 hours and collected warm on a 0.45 μm nylon filter, washed 2 × 100 mL portions of RO water, and air dried. The crude Bunte salt was resuspended
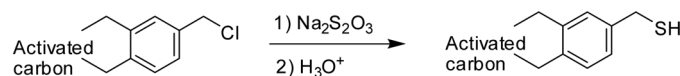

FIG. 2. A generic schematic showing the incorporation of thiols onto an activated carbon backbone.

in 100 mL of 3.0 N HCl and the mixture was held in a sealed Mason jar at 80°C for 12 hours (14). The suspension was stirred for 1 hour and returned to a temperature of 80°C for an additional hour before being filtered through a medium glass frit. The collected AC-CH$_2$-SH was washed with 2×100 mL portions of RO water, followed by a 100 mL portion of methanol. The washed material was dried in vacuo at 0.75 atm. for 18 hours at 25°C to yield 1.78 g of material. Elemental analysis of the product revealed a S content of 1.88%. This corresponds to 0.59 mmoles thiol per gram of sorbent. Given that the intermediate thiosulfate has a functional density of 0.65 mmole/g, this result indicates that the hydrolysis reaction proceeded cleanly and in >90% yield. BET surface area analysis revealed a surface area to mass ratio of 1244 m^2/g, with a pore volume of 1.29 cc/g. There was no discernable difference in the pore size distribution from the chloromethylated activated carbon starting material. FTIR analysis of the thiol-methylated material was inconclusive in terms of identifying new bands for the −CH$_2$−SH group (the thiol S−H stretch at ∼2550 cm^{-1} is typically very weak, and is commonly undetected (15)).

K$_d$ Measurements

For distribution coefficient (K$_d$) measurements, the filtered river water (from Columbia River, Richland, WA) was spiked with metal ions (Co^{2+}, Cu^{2+}, As^{3+}, Ag$^+$, Cd^{2+}, Hg^{2+}, Tl$^+$, and Pb^{2+}) to obtain 100 µg/L each. The solution pH was adjusted to the desired values using 0.1 M HNO$_3$ and 0.1 M NaOH. After 30 min of incubation, it was aliquoted into 4.9 mL volumes in a 20 mL polypropylene vial. The solution was then spiked with 0.1 mL of a suspension of solid sorbent and deionized distilled (DI) water at liquid per solid ratio (L/S in the unit of mL/g throughout) of 100. This resulted in a final L/S of 5,000. The control was performed in the same fashion but without solid sorbent. The sample was then shaken for 2 hrs at 160 rpm on an orbital shaker. After 2 hrs, the solution was removed by filtering thru 0.45-µm syringe Nylon-membrane filters and the filtrate was kept in 2 vol.% HNO$_3$ prior to metal analysis. The concentrations in the control (no sorbent) and the test solutions (after being contacted with a sorbent material) were analyzed using an inductively coupled plasma-mass spectrometer (ICP-MS, Agilent 7500ce, Agilent Technologies, CA). All batch experiments were performed in triplicates and the averaged values were reported. K$_d$ (in the unit of mL/g throughout) is simply a mass-weighted partition coefficient between the solid phase and the liquid supernatant phase as follows:

$$K_d = \frac{(C_o - C_f)}{C_f} \times \frac{V}{M} \quad (1)$$

where C$_o$ and C$_f$ are the initial and final concentrations in the solution of the target species determined by ICP-MS, V

is the solution volume in mL, and M is the mass in gram of the sorbent.

Sorption Capacity

The sorption capacity of sorbents for metal ions was measured in the same fashion as with the K$_d$, but only a single element was used and its concentration was varied in the solution until maximum sorption capacity was obtained. This was accomplished by using a large excess of metal ions to the number of binding sites on the sorbent materials (e.g., 0.1 to 4 mg/L of metal ion at L/S of 100,000).

Sorption Kinetics

The kinetics of metal sorption was performed in the same fashion as with the equilibrium studies except that 1 mL of well-mixed aliquot was removed and filtered at 0, 1, 2, 5, 10, 30, 60 min, 4, 7, and 24 hr and the initial sample volume was increased to 100 mL to minimize the change in L/S.

RESULTS AND DISCUSSION

Chloromethylation of the activated carbon was found to proceed smoothly. The starting activated carbon had a specific surface area of 1483 m^2/g. The chloromethylated product was found to have a specific surface area of 1310 m^2/g. If the absolute surface area of the material remained constant, then one would expect the surface area to mass ratio to drop since the system had gained mass (loss of a H$^+$ and gain of a −CH$_2$Cl group at each substitution site). A modest mass increase was observed in the chloromethylation reaction (∼17%), and if the absolute surface area were fixed then the predicted surface area to mass ratio would be 1223 m^2/g. While the agreement is not perfect, this observation supports the conclusion that the chloromethylation reaction did not significantly impact the surface area of the carbon substrate. Consistent with this, the pore volume was observed to drop slightly from 1.53 cc/g to 1.30 cc/g. The observed isotherm (see Fig. 3) and pore size distribution (see Fig. 4) of the product indicate that there was no significant crosslinking or pore blockage of the activated carbon taking place during the chloromethylation reaction under these conditions. The chloride content of this material (∼1.46 mmole/g) indicates that the degree of chloromethylation of this material under these conditions is similar to the original Merrifield synthesis (4). This chloromethylated activated carbon can be thought of as an analog to Merrifield's resin, except that it has a rigid, open, nanoporous architecture. Whereas Merrifield's resin is swellable, this chloromethylated activated carbon is not, and while much of the use of Merrifield's resin involves the "external" functionality (e.g., in peptide synthesis), much of the functionality of this chloromethylated activated carbon is internal (which may
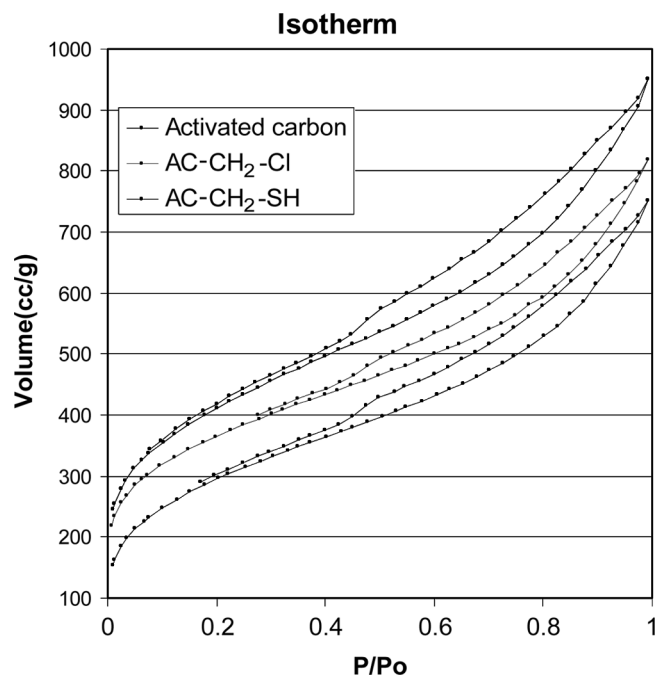
Isotherm

FIG. 3. Adsorption isotherms for activated carbon (Darco KB-B; Aldrich; top), chloromethylated activated carbon (AC-CH$_2$Cl; middle), and thiol-methylated activated carbon (AC-CH$_2$-SH; bottom).

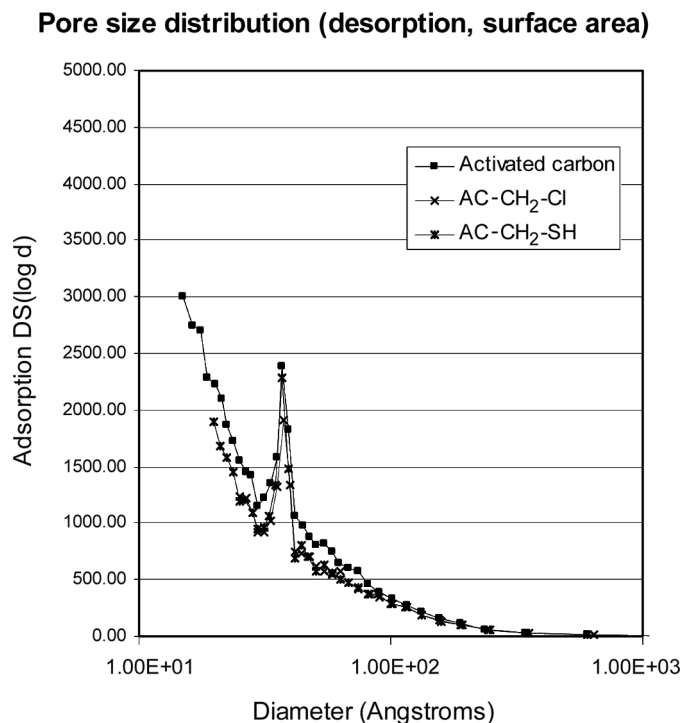## Pore size distribution (desorption, surface area)

FIG. 4. Pore size distributions for the activated carbon (Darco KB-B; Aldrich; top), chloromethylated activated carbon (AC-CH$_2$Cl), and thiol-methylated activated carbon (AC-CH$_2$-SH).

prove useful for size-based separations). One other key difference is the stability of the activated carbon backbone vs. the polystyrene backbone; activated carbon has clear advantages over polystyrene in terms of both thermal and chemical stability. It is anticipated that chloromethylated activated carbon will prove useful for a wide variety of applications, particularly for heavy metal separations and catalyst supports.

A similar chloromethylation reaction was attempted using phosphoric acid as solvent and both the Cl content and surface area of that product were much lower.

Not surprisingly, the S$_N$2 displacement of the benzylic chloride with thiosulfate anion proceeded in reasonable yield, to afford the corresponding Bunte salt. The starting chloromethylated activated carbon contained 1.46 mmole/g of Cl, while the thiosulfate was found to contain only 0.65 mmole/g of thiosulfate. Elemental analysis of the thiosulfate product revealed only 0.15% Cl, indicating >97% of the benzylic chloride had been consumed. Since only ~45% of the benzylic chloride was converted to the corresponding thiosulfate, the remainder must have been consumed in some other competing process (solvolysis in the refluxing aqueous methanol?).

In contrast to the chloromethylation step, the displacement of chloride by thiosulfate anion does not impose any chemical change on the carbon backbone, only on the pendant chloromethyl group. Therefore, it seems reasonable to predict that there should be little morphological change to the substrate itself. The chloromethylated activated carbon had a specific surface area of 1310 m^2/g and the product after treatment with thiosulfate had a specific surface area of 1179 m^2/g. If the absolute surface area of the material remained constant during this reaction, then one would expect the surface area to mass ratio to go down with the displacement of chloride (atomic weight of 35.5 g/mole) by the heavier sodium thiosulfate moiety (NaS$_2$O$_3$, MW = 135.2 g/mole) since the system would be increasing in mass. For ~50% conversion with ~1.5 mmole/g, this would predict a specific surface area of ~1250 m^2/g (ignoring the fate of the other half of the −CH$_2$Cl groups). Once again, while the fit is not exact, the trend is in the right direction, and it supports the conclusion that there was no significant change to the morphology of the carbon backbone during this displacement reaction.

Thiosulfates are known to be cleanly and quantitatively cleaved to the corresponding thiol under acidic conditions (14). Therefore, a batch of the crude thiosulfated activated carbon was subjected to hydrolysis using 3 M HCl at 80°C overnight. This produced the corresponding thiol cleanly and in high yield. The thiol was found to have a specific surface area of 1244 m^2/g, a pore volume of 1.29 cc/g and a sulfur content of 1.88% (corresponding to 0.59 mmole thiol per gram of sorbent). The adsorption isotherm and pore size distribution support the conclusion that there

was no significant change to the pore structure during the thiosulfate hydrolysis (see Figs. 3 and 4).

In order to assess the chemical utility of this new thiol-methylated activated carbon (which we will abbreviate AC-CH$_2$-SH), we carried out a series of sorption experiments with a variety of metal cations, under a range of pH conditions. The results are summarized in Table 1.

For the sake of comparison, a parallel series of experiments was also carried out using thiol terminated self-assembled monolayers on mesoporous supports (thiol-SAMMS$^{®}$) (16) to see what effect (if any) the nature of the backbone had on the performance of these thiol sorbents. A series of control experiments was also carried out with unmodified activated carbon.

The first trend apparent from these data are that both the AC-CH$_2$-SH and thiol SAMMS$^{®}$ sorbent systems are very effective for capturing Hg (our primary target) across a wide range of pH. Under most conditions, the AC-CH$_2$-SH had lower affinity for Hg, Ag, Cd and Cu relative to SAMMS$^{®}$. This is presumably due to the fact that the dense packing of thiol groups in the organized monolayer environment of SAMMS$^{®}$ allows for multiple metal ligand interactions, and hence a greater binding affinity (17). In the AC-CH$_2$-SH there is no such order, and the binding affinity is more likely a reflection of isolated thiol groups interacting with the metal cations.

The low binding affinity for Tl(I) is surprising. Tl(I) is almost as "soft" as Hg (18), and would be predicted to bind almost as strongly to the thiol group of AC-CH$_2$-SH as Hg. However, as can be seen from the data in Table 1, very little Tl(I) binding was observed. One possible explanation for this would be the interaction of As(III) (i.e., arsenious acid) with the Tl(I) cation. Arsenious acid is known to coordinate to "soft" Lewis acids (e.g., Pd (19)), lending some credence to this hypothesis. Why the As(III) would selectively bind the Tl(I) in the presence of these other metal cations isn't clear at this point.

As was observed with thiol SAMMS$^{®}$, heavy metal binding affinity was found to increase with increasing pH, especially for Hg (our primary target), suggesting perhaps that this sorbent may find application for heavy metal capture under strongly alkaline conditions where silica or polymer-based sorbents may be unstable. It is important to recognize that while this activated carbon has been decorated with thiol groups, the other "indigenous" functionality that was already present was not "erased" (i.e., the carboxylic acids, phenols, lactones, etc. (20)). The increased metal binding with increasing pH is particularly pronounced for Hg, Cu, Ag, and Pb once the pH gets above about 6, which correlates approximately with the pKa of the phenolic −OH group, so it may be due to the deprotonation of phenols, and subsequent interaction of the phenoxide anion with the metal cations. Using the data from the AC experiments for reference, it is clear that this phenoxide mechanism is not the primary driver for the metal binding, suggesting that perhaps there might be some sort of ligand

TABLE 1

Heavy metal sorption experiments using thiolated activated carbon (AC-CH$_2$-SH). All experiments were performed in triplicate and averaged

Sorbent	Final pH	Average K_d (mL/g sorbent)							
		Co(II)	Cu(II)	As(III)	Ag(I)	Cd(II)	Hg(II)	Tl(I)	Pb(II)
SH-SAMMS	0.11	170	180	27000	2600000	65	1500000	29	31
	2.01	0	74000	7100	3300000	0	1400000	15	22
	4.13	23	210000	1000	2800000	310	1500000	140	250
	6.19	170	140000	5800	1100000	4400000	810000	150	630000
	7.35	650	250000	16000	640000	1600000	650000	400	2700000
	8.31	870	280000	18000	440000	1100000	550000	340	1900000
AC-CH$_2$SH	0.17	280	260	180	1700	0	1600000	96	91
	2.02	160	260	78	1400	83	1100000	19	120
	4.31	120	2100	0	5800	270	1800000	110	1500
	6.37	1100	55000	160	62000	1400	2200000	560	86000
	7.33	1900	100000	0	340000	5000	6100000	1500	120000
	8.49	2100	88000	0	410000	4300	20000000	1700	110000
Activated carbon	2.12	0	55	0	220	0	2600	73	170
	4.22	110	5400	0	820	170	4800	250	6600
	7.61	1300	53000	23	3400	2900	9700	1800	67000

Initial metal conc = 100 ppb each, L/S = 5000, in pH-adjusted filtered river water.

synergy between the thiolate and the phenolate ligands under these alkaline conditions.

Kinetics

In order to probe the kinetics of Hg sorption, a kinetics experiment was carried using a 1,000 ppb solution of Hg(II) at a nominal pH of 5. The results are summarized in Fig. 5. This experiment was carried out with a liquid/solid ratio of 1,000. As can be seen from the data, the Hg sorption kinetics using AC-CH$_2$-SH are quite rapid, taking the Hg concentration down to ~0.04 ppb in less than 30 minutes. While this is significantly faster than the commonly-used Hg sorbents (e.g., GT-73 (16,21), or sulfur-impregnated activated carbon (22)), it is notably slower than thiol-SAMMS®, which achieves similar results in just 2–3 minutes under similar conditions (16,21).

Hg Capacity

A series of experiments were carried out to determine the Hg binding capacity of AC-CH$_2$-SH. These experiments were carried out with a solution/solids ratio of 100,000, and at a nominal pH of 5.5. As can be seen from the results summarized in Fig. 6, the data display Langmuirian behavior, and reveal a binding capacity of approximately 33 mg Hg per gram of sorbent. This is much smaller capacity than the >600 mg Hg per g sorbent that has been observed with thiol-SAMMS® (21).

The Hg binding capacity of the AC-CH$_2$-SH is a small fraction of the observed level of functionalization (0.165 mmole Hg per gram sorbent, compared with 0.59 mmole thiol per gram of sorbent). Assuming a 1:1 binding stoichiometry, this corresponds to about 28% of the thiol loading, suggesting that much of the thiol functionality is not easily accessible to solution-borne metal ions. A similar observation has been noted before with other functional groups (2,3). Activated carbon commonly
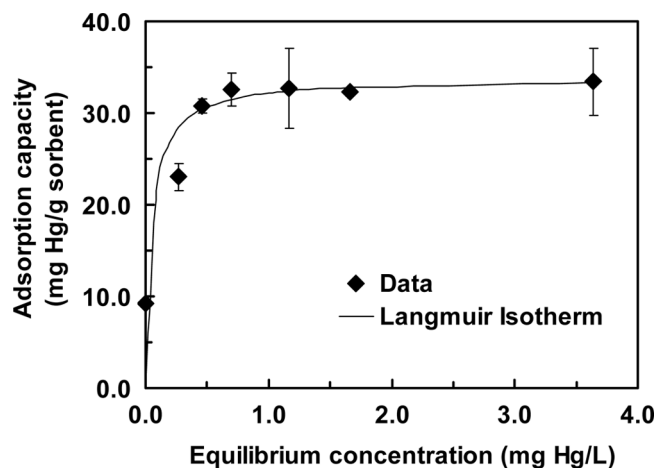
FIG. 6. Absorption capacity isotherm for Hg onto AC-CH$_2$-SH at pH of ~5.5.

has a great deal of microporosity, and it may well be that much of the functionality is anchored inside these micropores, making it kinetically inaccessible. Another possible explanation would be multiple thiol/metal interactions (e.g., a 2:1 or 3:1 binding stoichiometry). This has been observed before in densely populated, more highly ordered systems (17), but is less likely in this more disordered system, with somewhat lower functional density.

The binding of Hg(II) by activated carbon is known to be dependant on the level of oxidation of the activated carbon, with Hg binding capacity going down with increasing oxidation of the carbon sorbent (23). The Hg(II) binding capacities reported for ozonized activated carbons are somewhat lower than we report here (e.g., 10–20 mg/g (23)), while other "unadulterated" activated carbons are similar (~25 mg/g (23)), and yet others have been reported to have much higher Hg binding capacities (e.g., 154 mg/g (24)). It has been proposed that the Hg binding by activated carbon is due to a redox mechanism arising from electron rich portions of the carbon backbone (23,24,26), and therefore the processing that the activated carbon has been subjected to is likely to be of critical importance. The limited role that this mechanism plays in our studies is readily apparent from the results summarized in Table 1 – the unmodified activated carbon has but a small fraction of the affinity for Hg(II) of the AC-CH$_2$-SH. This particular activated carbon has an oxygen content of 12.7%, making it fairly highly oxidized in the context of the discussion above, and hence a poor partner for the redox binding mechanism. Therefore, we conclude that the AC-CH$_2$-SH is binding the Hg primarily through the thiol group, via a covalent Hg-S bond.

If a significant portion of the −CH$_2$SH groups are indeed in kinetically inaccessible micropores, then that raises the question of how this chemistry might be
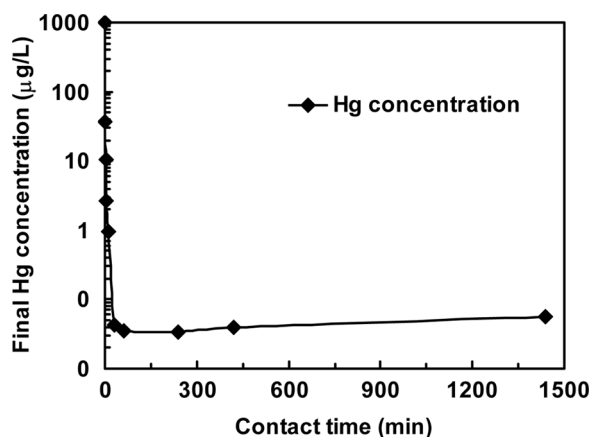
FIG. 5. Kinetics of Hg sorption by AC-CH$_2$-SH at pH ~5 (solution/solids ratio = 1,000).

improved upon. Obviously, larger pore carbons would be advantageous. One intriguing possibility would be the use of templated mesoporous carbons as the substrate to perform the chloromethylation reaction on since this would allow pore diameter to be dictated a priori. The success of this strategy will likely depend on the number of "edges" exposed in the carbon mesopores. Since this chemistry is based on an electrophilic aromatic substitution, there must be an aromatic C—H bond (i.e., the "edge" of an aromatic ring) exposed on the pore wall so the —CH$_2$Cl group can be installed. For the templated mesoporous carbons, this in turn suggests that the carbonization conditions chosen will likely play a critical role in the success or failure of this approach since the degree of graphitization of the pore walls will have a major impact on the number of C—H bonds remaining on the pore wall.

CONCLUSIONS

Chloromethylated activated carbon is easily made from cheap, readily available materials. The level of chloromethylation observed is similar to that reported in the original synthesis of Merrifield's resin. The chloromethylation reaction does not seem to have any negative impact on the surface area or pore structure of the activated carbon. The benzylic Cl is readily displaced by nucleophiles, affording easy access to chemically modified activated carbons that are useful for chemical separations. We have exploited this to make activated carbon that has been decorated with thiol groups, and shown that it is useful as a heavy metal sorbent. AC-CH$_2$-SH was found to be fast, effective, and easily capable of reducing Hg concentrations down to well below ppb levels (e.g., 0.04 ppb) and binds the Hg via a strong covalent Hg-S bond. The Hg sorption kinetics of AC-CH$_2$-SH are much faster than those observed for currently used conventional sorbents (e.g., GT-73 or sulfur-impregnated activated carbon). The activated carbon backbone provides excellent chemical and thermal stability to the AC-CH$_2$-SH sorbent, and has been shown to enhance the sorbent's affinity for heavy metals under alkaline conditions. Hg binding capacity measurements using AC-CH$_2$-SH suggest that a significant portion of the thiol groups may be in kinetically inaccessible micropores.

AC-CH$_2$-SH is not as powerful a Hg sorbent as thiol-SAMMS®. Thiol SAMMS® not only displays significantly faster sorption kinetics, but also a much higher Hg binding capacity. However, AC-CH$_2$-SH may well prove useful under conditions where silica-based sorbents are not well-suited (e.g., strongly alkaline conditions). Further studies are underway with these, and related materials.

ACKNOWLEDGEMENTS

REFERENCES

1. Sinha, R.K.; Walker, P.L., Jr. (1972) Removal of mercury by sulfurized carbons. *Carbon*, 10 (6): 754–756.
2. Yantasee, W.; Lin, Y.; Fryxell, G.E.; Alford, K.L.; Busche, B.J.; Zemanian, T. S. (2004) Selective removal of copper(II) from aqueous solutions using fine-grained activated carbon functionalized with amine. *Ind. Eng. Chem. Res.*, 43 (11): 2759–2764.
3. Yantasee, W.; Lin, Y.; Fryxell, G.E.; Alford, K.L.; Busche, B.J.; Johnson, C.D. (2004) Electrophilic aromatic substitutions of amine and sulfonate onto fine-grained activated carbon for aqueous-phase metal ion removal. *Sep. Sci. & Technol.*, 39 (14): 3263–3279.
4. Merrifield, R.B. (1963) Solid phase peptide synthesis. I. The synthesis of a tetrapeptide. *J. Am. Chem. Soc.*, 85 (14): 2149–2154.
5. Crowley, J.I.; Rapoport, H. (1976) Solid-phase organic synthesis: Novelty or fundamental concept? *Acc. Chem. Res.*, 9 (4): 135–144.
6. Leznoff, C.C. (1978) The use of insoluble polymer supports in general organic synthesis. *Acc. Chem. Res.*, 11 (9): 327–333.
7. Booth, R.J.; Hodges, J.C. (1997) Polymer-supported quenching reagents for parallel purification. *J. Am. Chem. Soc.*, 119 (21): 4882–4886.
8. See, for example, the latest Aldrich catalog for the varieties of Merrifield's resin that are currently commercially available.
9. March, J. (1992) *Advanced Organic Chemistry*, 4th Ed.; Wiley-Interscience: New York, 550.
10. For an excellent summary of the structure and properties of activated carbons, see. Bansal, R.C.; Goyal, M. (2005) *Activated Carbon Adsorption*; Taylor & Francis: New York, 1–51.
11. Fryxell, G.E.; Mattigod, S.V.; Lin, Y.; Wu, H.; Fiskum, S.; Parker, K.; Zheng, F.; Yantasee, W.; Zemanian, T.S.; Addleman, R.S.; Liu, J.; Kemner, K.; Kelly, S.; Feng, X. (2007) Design and synthesis of self-assembled monolayers on mesoporous supports (SAMMS): The importance of ligand posture in functional nanomaterials. *J. Mater. Chem.*, 17 (28): 2863–2874.
12. (a) Grummitt, O.; Buck, A. (1955) 1-Chloromethylnaphthalene. Organic Syntheses, Collective Volume 3, 195; (b) Wiberg, K.B.; McShane, H.F. (1955) 2-Chloromethylthiophene. Organic Syntheses, Collective Volume 3, 197; (c) Reynold, C.; Fuson, R.C.; Rabjohn, N. (1955) Mesitylacetic acid. Organic Syntheses, Collective Volume 3, 557.
13. Distler, H. (1967) The chemistry of bunte salts. *Angew. Chem. Internat. Eng. Edit.*, 6 (6): 544–553.
14. Kice, J.L. (1963) A kinetic study of the acid hydrolysis of a Bunte salt. *J. Org. Chem.*, 28 (4): 957–961.
15. Silverstein, R.M.; Webster, F.X.; Kiemle, D.J. (2005) *Spectrometric Identification of Organic Compounds*, 7th Ed.; John Wiley & Sons: Hoboken, NJ, 105.
16. (a) Feng, X.; Fryxell, G.E.; Wang, L.Q.; Kim, A.Y.; Liu, J. (1997) Hybrid mesoporous materials with functionalized monolayers. *Science*, 276 (#5314): 923–926; (b) Liu, J.; Feng, X.; Fryxell, G.E.; Wang, L.Q.; Kim, A.Y.; Gong, M. (1998) Hybrid mesoporous materials with functionalized monolayers. *Adv. Mater.*, 10 (2): 161–165.
17. Fryxell, G.E. (2007) Synthesis of nanostructured hybrid sorbent materials using organosilane self-assembly on mesoporous ceramic oxides. In: *Environmental Applications of Nanomaterials: Synthesis, Sorbents and Sensors*, Fryxell, G.E.; Cao, G., eds.; Imperial College Press: Singapore, 159.

18. Misono, M.; Ochiai, E.; Saito, Y.; Yoneda, Y. (1967) A new dual parameter scale for the strength of Lewis acids and bases with the evaluation of their softness. *J. Inorg. & Nucl. Chem.*, *29* (11): 2685–2691.

19. Sokolov, M.N.; Virovets, A.V.; Dybtsev, D.N.; Chubarova, E.V.; Fedin, V.P.; Fenske, D. (2001) Phosphorous acid and arsenious acid as ligands. *Inorg. Chem.*, *40* (19): 4816–4817.

20. Bansal, R.C.; Goyal, M. (2005) *Activated Carbon Adsorption*; Taylor & Francis: New York, 10.

21. (a) Chen, X.; Feng, X.; Liu, J.; Fryxell, G.E.; Gong, M. (1999) Mercury separation and immobilization using self-assembled monolayers on mesoporous supports (SAMMS). *Sep. Sci. & Technol.*, *34* (6&7): 1121–1132; (b) Mattigod, S.V.; Feng, X.; Fryxell, G.E.; Liu, J.; Gong, M. (1999) Separation of complexed mercury from aqueous wastes using self-assembled mercaptan on mesoporous silica. *Sep. Sci. & Technol.*, *34* (12): 2329–2345.

22. Shin, Y.; Fryxell, G.E.; Um, W.; Parker, K.; Mattigod, S.V.; Skaggs, R. (2007) Sulfur-functionalized mesoporous carbon. *Adv. Funct. Mater.*, *17* (15): 2897–2901.

23. Sanchez-Polo, M.; Rivera-Utrilla, J. (2002) Adsorbent−adsorbate interactions in the adsorption of Cd(II) and Hg(II) on ozonized activated carbons. *Environ. Sci. & Technol.*, *36* (17): 3850–3854.

24. Namasivayam, C.; Kadirvelu, K. (1999) Uptake of mercury (II) from wastewater by activated carbon from an unwanted agricultural solid by-product: Coirpith. *Carbon*, *37* (1): 79–84.

25. Lopez-Gonzalez, J.D.; Moreno-Castilla, C.; Guerrero-Ruiz, A.; Rodriguez-Reinoso, F. (1982) Effect of carbon-oxygen and carbon-sulphur surface complexes on the adsorption of mercuric chloride in aqueous solutions by activated carbons. *J. Chem. Technol. Biotechnol.*, *32* (5): 575–579.

26. Rivin, D. (1971) Surface properties of carbon. *Rubber Chem. Technol.*, *44* (2): 307–343.